3102 *Chem. Mater.* **2009,** *21,* 3102–3109
DOI:10.1021/cm900204q

CHEMISTRY OF MATERIALS
Article

Surface, Interface, and Bulk Structure of Borate Containing Apatitic Biomaterials

Sabrina Barheine,[†] Satoshi Hayakawa,[‡] Akiyoshi Osaka,[‡] and Christian Jaeger*[,†]

[†]*BAM Federal Institute for Materials Research and Testing, Division I.3, Richard-Willstaetter-Str. 11, D-12489 Berlin, Germany, and* [‡]*Biomaterials Laboratory, Graduate School of Natural Science and Technology, Okayama University, 3-1-1, Tsushima, Okayama 700-8530, Japan*

Received January 22, 2009. Revised Manuscript Received May 20, 2009

Nuclear magnetic resonance (NMR) has been used for a detailed investigation of the borate incorporation in apatitic biomaterials prepared by high-temperature solid-state reaction sintering. The NMR data clearly show that crystalline hydroxyapatite (HAp) does exist, but it contains only about 30% of the entire phosphate content of the sample. The main phosphate content of about 70% forms a disordered calcium phosphate phase (BCaP) that accommodates the borate units in two structurally different trigonal BO_3^{3-} groups besides some minor linear BO_2^- units. The average chemical composition of BCaP was estimated from the NMR spectra. Furthermore, a structural model of these particles is proposed, where HAp forms the crystalline core of these crystals covered by the disordered BCaP, suggesting that the BCaP phase is responsible for the adhesion properties of organic molecules like proteins and not HAp that is the only significant crystalline phase (XRD). Furthermore, the presence of an interface between HAp and BCaP is discussed based on various NMR experiments, including a triple-resonant $^{11}B-^{31}P$ cross-polarization edited ^{31}P NMR spectrum with subsequent $^{31}P\{^1H\}$ REDOR (Rotational Echo DOuble Resonance) dephasing.

1. Introduction

Many of clinically available synthetic bone substitutes are calcium phosphate ceramics such as hydroxyapatite (HAp).[1] HAp has been used as a scaffold of growth factors for bone regeneration.[2] Calcium phosphate particles also serve as carriers for controlled protein release for bone regeneration[3] or for antibiotics for biodegradable bone implants[4] and are used for cell transfection in biochemical applications.[5] Protein release from HAp particles results among other features from the HAp dissolution rate.[4] For this reason, various kinds of cations[6] and anions[7,8] have been used as substituents for Ca^{2+}, PO_4^{3-}, or OH^- ions in the HAp lattice. Regarding the adsorption of basic proteins (such as growth factors) or the rate of dissolution, anion substitutions such as borate,[9] carbonate,[7] and silicate ions[8] for negatively charged PO_4^{3-} groups and OH^- sites in the HAp lattice must control both electrostatic interactions and chemical bonding between the phosphate particle and the basic proteins as well as the solubility of substituted apatite in our body environment.

Previous studies reported that if borate is introduced into a HAp lattice, phosphate anions and OH^- groups can be partially substituted by planar BO_3^{3-} and linear BO_2^- units, respectively, leading to AB-type borohydroxyapatite.[9−12] However, only a single XRD single crystal study exists in the literature which describes the location of linear BO_2^- groups in apatitic calcium phosphate.[11] No XRD evidence is available so far concerning the location of trigonal BO_3^{3-} groups in calcium phosphates.

Therefore, the main question that remains open is how a calcium phosphate structure (not necessarily HAp) can accommodate borate units, because the discussed insertion of a planar BO_3^{3-} group either at a phosphate place (tetrahedral unit) or an OH^- unit must cause significant lattice distortions due to the different sizes and shapes of the various groups. In addition, cations must be rearranged in close spatial proximity to ensure electric

*Corresponding author. E-mail: christian.jaeger@bam.de.

(1) Daculsi, G. *Biomaterials* **1998**, *19*, 1473.
(2) Okubo, Y.; Bessho, K.; Fujimura, K.; Kusumoto, K.; Ogawa, Y.; Iizuka, T. *Clin. Orthop.* **2000**, *375*, 295. Ono, I.; Ohura, T.; Miura, M.; Yamaguchi, H.; Ohnuma, Y.; Kuboki, Y. *Plast. Reconstr. Surg.* **1992**, *90*, 870.
(3) Matsumoto, T.; Okazaki, M.; Inoue, M.; Yamaguchi, S. Kusunose, T.; Toyonaga, T.; Hamada, Y.; Takahashi, J. *Biomaterials* **2004**, *25*, 3807.
(4) Tadic, D.; Welzel, T.; Seidel, P.; Wüst, E.; Dingeldein, E.; Epple, M. *Materialwiss. Werkstofftech.* **2004**, *35*, 1002.
(5) Jordan, M.; Wurm, F. *Methods* **2004**, *33*, 136.
(6) Fujii, E.; Ohkubo, M.; Tsuru, K.; Hayakawa, S.; Osaka, A.; Kawabata, K.; Bonhomme, C.; Babonneau, F. *Acta Biomater.* **2006**, *2*, 69. Hayakawa, S.; Ando, K.; Tsuru, K.; Osaka, A.; Fujii, E.; Kawabata, K.; Bonhomme, C.; Babonneau, F. *J. Am. Ceram. Soc.* **2007**, *90*, 565.
(7) Takemoto, S.; Kusudo, Y.; Tsuru, K.; Hayakawa, S.; Osaka, A.; Takashima, S. *J. Biomed. Mater. Res.* **2004**, *69A*, 544.
(8) Gasquères, G.; Bonhomme, C.; Maquet, J.; Babonneau, F.; Hayakawa, S.; Kanaya, T.; Osaka, A. *Magn. Reson. Chem.* **2008**, *46*, 342.
(9) Ternane, R.; Cohen-Adad, M. Th.; Panzer, G.; Goutaudier, C.; Kbir-Ariguib, N.; Trabelsi-Ayedi, M.; Florian, P.; Massiot, D. *J. Alloys Compd.* **2002**, *333*, 62.
(10) Calvo, C.; Faggiani, R. *J. Chem. Soc., Chem. Commun.* **1974**, 714.
(11) Ito, A.; Aoki, H.; Miura, N.; Otsuka, R.; Tsutsumi, S. *J. Ceram. Soc. Jpn.* **1988**, *96*, 305.
(12) Hayakawa, S.; Sakai, A.; Tsuru, K.; Osaka, A.; Fujii, E.; Kawabata, K.; Jaeger, C. *Key Eng. Mater.* **2008**, *361*, 191.

Published on Web 07/06/2009

neutrality. As a result the local molecular structure around the discussed substitution sites must be altered severely, and a new structure, different from HAp, must arise. It has been described by Ito et al.[11] as the authors mention explicitly that if linear BO_2^- groups are incorporated instead of OH^- the new structure is "apatitic in character".

In our view, this lack of precise structure information regarding the borate incorporation combined with the fact that often only HAp is found by XRD in such borate containing samples has led to the view that HAp is the host lattice in which trigonal BO_3^{3-} units may replace the PO_4^{3-} and/or OH^- sites. The aim of this paper is to improve the knowledge about this important issue in more detail using two-dimensional (2D) and double-resonant Nuclear Magnetic Resonance (NMR) experiments. The present study was also triggered by a previous NMR investigation of nanocrystalline HAp samples[13] which showed that only about half of the entire phosphate content is found in stoichiometric HAp forming the core of the nanoparticles. The residual phosphate forms a thin amorphous surface layer with a different chemical composition. This model explains the observed Ca^{2+} deficiency of such nanocrystalline HAp samples and is by now supported in the literature.[14]

Using this NMR concept, the focus is on (i) the verification that a second borate containing calcium phosphate (BCaP) phase exists besides crystalline HAp, (ii) the determination of the phosphate content in the XRD evident HAp phase and the estimation of the chemical composition of the BCaP phase, and (iii) the suggestion that HAp forms the core of the crystals covered by the disordered BCaP phase—a key result for understanding the interaction of such materials with organic molecules such as proteins or polysaccharides.

2. Experimental Section

2.1. Sample Preparation. Boron containing calcium orthophosphate (synthesis composition: $10CaO \cdot 5.5PO_{2.5} \cdot 0.5BO_{1.5}$; formally recalculated according to the ICP data (cf. Supporting Information: $10.46CaO \cdot 5.72PO_{2.5} \cdot 0.47BO_{1.5}$) was prepared by solid-state reaction sintering process using $CaCO_3$, $(NH_4)_2HPO_4$, and H_3BO_3 as described by Ternane et al.[15] The starting materials were mixed in an alumina mortar for 1 h and then pressed into pellets and put in a platinum crucible. After heating up at a rate of 5 K min^{-1}, they were kept at 1673 K for 6 h in an electric furnace, cooled to room temperature, and powdered in an alumina mortar for 1 h. This procedure was repeated a second time to produce homogeneous particles. Further information including ICP, FT-IR, and XRD analysis is available in the Supporting Information

2.2. NMR. NMR experiments were performed on a Bruker Avance 600 spectrometer (Bruker Biospin GmbH, Rheinstetten, Germany, $B_0 = 14.1$ T) operating at ^1H, ^{31}P, and ^{11}B frequencies of 600.1, 242.92, and 192.54 MHz, respectively using a triple resonance 4 mm H/X/Y MAS probe. The spinning rate was 12.5 kHz. The chemical shifts are referenced using secondary solid standard samples (easier to handle and narrow MAS lines for a correct chemical shift calibration) which were referenced earlier against common liquid reference standards. A well crystalline HAp sample was used as solid standard setting the single ^1H and ^{31}P resonances to $\delta(^1H) = 1.78$ ppm (against TMS) and $\delta(^{31}P) = 2.3$ ppm (against 85% phosphoric acid solution), whereas the narrow ^{11}B MAS NMR signal of solid BPO_4 at $\delta(^{11}B) = -4.1$ ppm (against $BF_3(Et_2O)$) was used for the ^{11}B chemical shift scale.

^1H MAS NMR spectra were recorded with a 90° pulse length of 3.6 μs, a recycle delay of 600 s, and four scans. ^{31}P MAS NMR spectra were acquired with a 90° pulse length of 5 μs, a recycle delay of 1800 s, and two scans after saturation. These long repetition times are required to avoid any saturation effects; for example, the ^{31}P T_1 is about 360 s, whereas the 7 ppm and 5 ppm ^1H lines have a T_1 of about 120 s. ^1H high power two-pulse phase modulation (TPPM) decoupling[16] was applied in the ^{31}P NMR measurements at $B_1 = 83.3$ kHz. ^{11}B MAS NMR spectra were recorded with a selective 90° pulse[17] of 2 μs (B_1 field: 62.5 kHz) and a recycle delay of 10 s and 1024 scans. The probe background was subtracted using separate measurements with an empty rotor under identical conditions.

2D $^1H-^{31}P$ heteronuclear correlation (HETCOR) experiments were performed using ramped (50% ramp on the ^1H channel) cross-polarization (CP)[18] with contact times of 2 and 8 ms, and a recycle delay of 80 s and 24 scans per t_1 increment. A total of 156 t_1 slices were acquired with 80 μs time delay corresponding to a rotor-synchronized incrementation in the indirect dimension using States method. The 90° ^1H pulse length was 3.3 μs. High power TPPM decoupling was applied (B_1 = 75.8 kHz).

2D $^{11}B-^{31}P$-HETCOR spectra were measured using CP with a contact time of 8 ms, a recycle delay of 8, and 448 scans per t_1 increment. A total of 64 t_1 slices were acquired with 80 μs time delay corresponding to a rotor-synchronized incrementation in the indirect dimension. The CP step in the experiment was performed with a selective ^{11}B 90° pulse length of 3.6 μs at a B_1 field of 34.5 kHz followed by the CP pulse using a 50% ramp on the ^{11}B channel (initial ^{11}B spin lock field of 2.5 kHz) and a constant ^{31}P B_1 field of 16.8 kHz.

The ^1H 90° and 180° pulse lengths for the $^1H\{^{11}B\}$ TRAPDOR (TRAnsfer of Population DOuble Resonance)[19] measurements were 3.8 and 7.6 μs (^1H B_1 field: 65.8 kHz), respectively, and the ^{11}B r.f. field strength was 90.9 kHz. Dephasing times of 2.56 ms (32 rotor cycles) and 5.76 ms (72 rotor cycles) were used. A total of 96 scans were acquired with a recycle delay of 16 s for this experiment.

Finally, $^{11}B-^{31}P$ CP edited $^{31}P\{^1H\}$ REDOR (Rotational Echo DOuble Resonance)[20] experiments were carried out with ^{31}P 90° and 180° pulse lengths of 4.7 and 9.4 μs, respectively, and ^1H 180° pulses of 6.6 μs during the REDOR. A total of 1024 scans were acquired with a recycle delay of 10 s for each experiment. The sample was restricted to the central part of the rotor to ensure maximum B_1 homogeneity. The $^{11}B-^{31}P$ CP

(13) Jäger, C.; Welzel, T.; Meyer-Zaika, W.; Epple, M. *Magn. Reson. Chem.* **2006**, *44*, 573.
(14) Bertinetti, L.; Drouet, C.; Combes, C.; Rey, C.; Tampien, A.; Coluccia, S.; Martra, G. *Langmuir* **2009**, *25*, 5647.
(15) Ternane, R.; Cohen-Adad, M. Th.; Bulon, G.; Florian, P.; Massiot, D. *Solid State Ionics* **2003**, *160*, 183.
(16) Bennett, A. E.; Rienstra, C. M.; Auger, M.; Lakshmi, K. V.; Griffin, R. G. *J. Chem. Phys.* **1995**, *103*, 6951.
(17) Schmidt, V. H. *Phys. Rev. B* **1973**, *7*, 4145.
(18) Metz, G.; Wu, X.; Smith, S. O. *J. Magn. Reson. Ser. A* **1994**, *110*, 219.
(19) Van Eck, E. R. H.; Janssen, R.; Maas, W. E. J. R.; Veeman, W. S. *Chem. Phys. Lett.* **1990**, *174*, 428.
(20) Guillion, T; Schaefer, J. *J. Magn. Reson.* **1989**, *81*, 196.

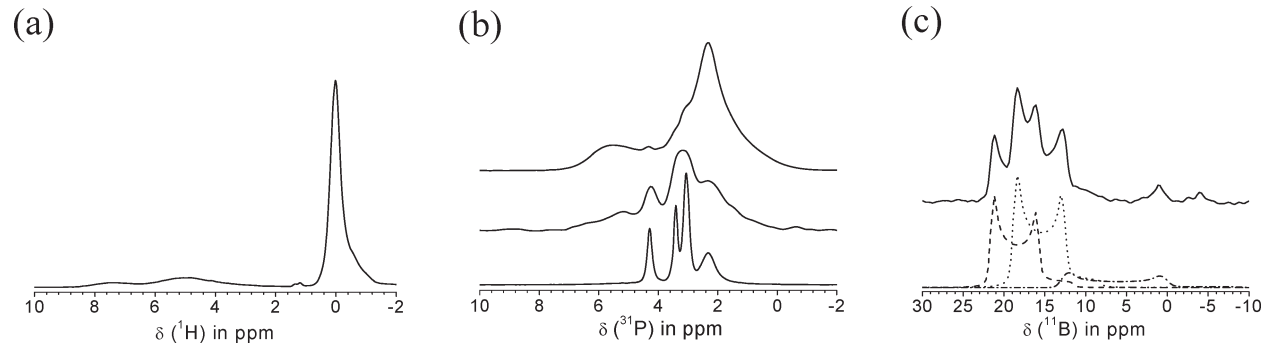

Figure 1. (a) ^{1}H MAS NMR spectrum of the sample. The main peak at 0 ppm is caused by the hydroxyl units of crystalline HAp. The high-field shoulder with its center at −0.6 ppm hints to additional Ca−OH type protons and will be discussed further below. In addition, few water and HPO_4^{2-} molecules are found (weak resonances at 5 ppm and 7.5 ppm, respectively). (b) ^{31}P NMR spectra: MAS spectrum (top) and rotor-synchronized delayed echo (echo delay of 80 ms or 100 rotor cycles) MAS spectrum (middle) of the sample; ^{31}P MAS spectrum of a TTCP ($Ca_4(PO_4)_2O$) reference compound (bottom) for comparison. For further details see text. (c) ^{11}B MAS NMR spectrum (top, solid line) and ^{11}B spectra simulations considering two BO_3^{3-} (dashed and dotted lines) and a BO_2^- unit (dash-dotted line). Line shape simulation was done using the DMfit software.[22]

step was the same as described above for the ^{11}B−^{31}P HETCOR NMR measurements.

3. Results and Discussion

This section is split into three parts because a patchwork of various NMR data hints as a whole to the suggested "core-shell" model of the material where the core consists of crystalline HAp covered by a disordered borate containing calcium phosphate (BCaP) phase. In the first two subsections it will be shown that HAp (as found in XRD) is not the only relevant structural phase. Clear evidence is given for the BCaP phase, and in section 3.2 its chemical composition is estimated from the NMR data. Finally and to support the model, special NMR experiments are used to get experimental evidence for an interface layer between HAp and BCaP (section 3.3).

3.1. ^{1}H, ^{31}P, and ^{11}B NMR spectra. The ^{1}H MAS NMR spectrum of the sample is shown in Figure 1a. It consists of a main resonance at 0 ppm, typical for the hydroxyl protons of the HAp structure. This result is consistent with XRD results.[12,21] However, this HAp signal at 0 ppm has a distinct high-field shoulder on the right caused by another, slightly broader line at −0.6 ppm (cf. Figure 5). Its chemical shift is very similar to that of the HAp OH^- protons, and we suggest that it is caused by a similar Ca−OH structural motif in a more disordered structure. Additionally, two weak ^{1}H signals are found at 7.5 ppm and 5 ppm which may be assigned to protons of few HPO_4^- units and water molecules, respectively, with a maximum proton content of less than about 10%.

The ^{31}P MAS NMR line shape (Figure 1b, top) is completely different from that of the crystalline HAp reference sample which consists of a single narrow line at 2.3 ppm (typical line width about 0.5 ppm). The spectrum shown at the top in Figure 1b consists of two broad peaks at 2.3 ppm and a smaller one at about 5.5 ppm. The 5.5 ppm peak has nothing in common with crystalline HAp, and also the 2.3 ppm resonance is much broader than HAp. Hence, the ^{31}P MAS NMR spectrum gives readily evidence for the presence of another calcium phosphate phase. However, HAp is present in this sample because the 2.3 ppm signal possesses a shape as if it consists of a narrower HAp signal at 2.3 ppm and a somewhat broader component directly underneath. It can be concluded form that line shape that the unknown phosphate phase contains a significant part of the total phosphate content, and it is obviously disordered because this phase does not show up in the XRD pattern. Additionally, the ^{31}P MAS NMR spectrum shows very small peaks at 4.4 ppm and 3.2 ppm. These peaks can be enhanced further using rotor-synchronized delayed echo data acquisition as shown in Figure 1b, middle (echo delay of 80 ms). These peaks belong unambiguously to tetracalcium phosphate (TTCP; $Ca_4(PO_4)_2O$) as shown by comparison to the ^{31}P MAS NMR spectrum of a reference sample (Figure 1b, bottom). About 1.7% of the entire phosphate is contained in TTCP determined from the line shape fit procedure.

The ^{11}B MAS NMR spectrum of the sample is shown in Figure 1c, top. Two different trigonal BO_3^{3-} units and few linear BO_2^- units are present in the sample, as shown by the line deconvolution (Figure 1c, bottom). The ^{11}B chemical shift and quadrupole parameters of these different BO_3^{3-} units and the linear BO_2^- are the same as reported previously.[9]

3.2. 1D and 2D NMR Spectra of BCaP and Estimation of Its Chemical Composition from the NMR Data. Cross-polarization (CP) transfer measurements can be used to probe spatial proximities between different nuclei, for example, between ^{1}H and ^{31}P or ^{11}B and ^{31}P. The corresponding ^{1}H−^{31}P CP and ^{11}B−^{31}P CP spectra are compared in Figure 2a (middle, bottom) with the ^{31}P MAS NMR line shape (top). The ^{1}H−^{31}P CPMAS spectrum shows now the typical narrow HAp line as expected from the XRD results, and it is clear that the overall 2.3 ppm peak of the ^{31}P MAS NMR spectrum must consist of two overlapped components, as suggested section 3.1. The line shape of the second, unknown component can be measured using ^{11}B−^{31}P CP as shown in Figure 2a, bottom. In other words, the ^{1}H−^{31}P CPMAS experiment detects the crystalline HAp phase, whereas the ^{11}B−^{31}P

(21) Barheine, S.; Hayakawa, S.; Osaka, A.; Jäger, C. *Key Eng. Mater.* **2009**, *396*, 205.

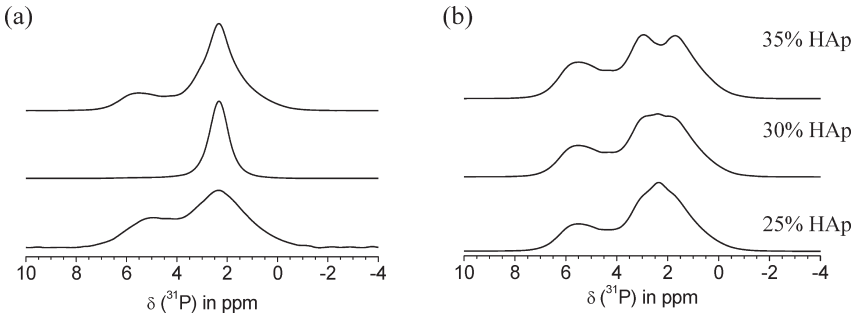

Figure 2. (a) ^{31}P MAS spectrum (top); ^{1}H−^{31}P CPMAS spectrum (middle) that shows the HAp resonance; ^{11}B−^{31}P CPMAS spectrum (bottom) of the BCaP phase in the sample. (b) Difference line shapes of the ^{31}P MAS NMR spectrum (part a, top) and differently scaled ^{1}H−^{31}P CPMAS spectra (part, a, middle) corresponding to relative phosphate contents in HAp of 35% (top), 30% (middle), and 25% (bottom). For more details see text.

CPMAS measurement excites the BCaP phase. It also means that the crystalline HAp (XRD verified) does not accommodate the borate groups!

Having these separate line shapes for the various phases it is now possible to determine the relative P content in HAp and BCaP. One possibility is to use the ^{31}P MAS and the ^{1}H−^{31}P CPMAS lines (Figure 2a, top and middle) provided that the CPMAS line shape does not depend on the CP time. This has been ensured by measuring various 2D ^{1}H−^{31}P correlation spectra (Figure 4) using different CP times. The line width of the 2D HAp ^{1}H−^{31}P correlation peak (cross section shown in Figure 4b, top) is constant. It should be noted that a similar observation has also been made previously[13] investigating nanocrystalline HAp. Hence, difference spectra between the ^{31}P MAS and (properly) scaled ^{1}H−^{31}P CPMAS lines can be calculated subtracting this way the HAp part from the entire spectrum. Figure 2b shows three difference line shapes corresponding to relative phosphate contents of HAp of 35% (top), 30% (middle), and 25% (bottom), respectively. The difference line shape assuming 35% phosphate in HAp shows a local minimum at 2.3 ppm; the line for 25% has a local maximum. Hence, it is unlikely that these two spectra represent the BCaP ^{31}P line shape. The most probable value seems to be around 30%. This simple estimation verifies that only about 30% of the phosphate is contained in the XRD detected HAp; about 70% forms the BCaP.[21] The phosphate/borate ratio for the entire sample is 12/1, as given in section 2.1 (ICP data); hence, if the 30 mol % phosphate in HAp ($Ca_{10}(PO_4)_6(OH)_2$) is subtracted from the total phosphate content, a phosphate/borate ratio for the remaining BCaP phase of ca. 8.3/1 follows. This ratio hints on a three-dimensional network where one borate unit is surrounded by about 8 phosphate units. Hence, one can assume that all phosphate sites of the unknown BCaP phase are excited in a ^{11}B−^{31}P CPMAS spectrum (Figure 2a, bottom). Thus, the ^{31}P line shape of the unknown BCaP consists of two broad peaks: one at 5 ppm and another one at 2.3 ppm. The latter resonance has the same chemical shift as crystalline HAp, but its line width is much larger! Furthermore, this broad 2.3 ppm

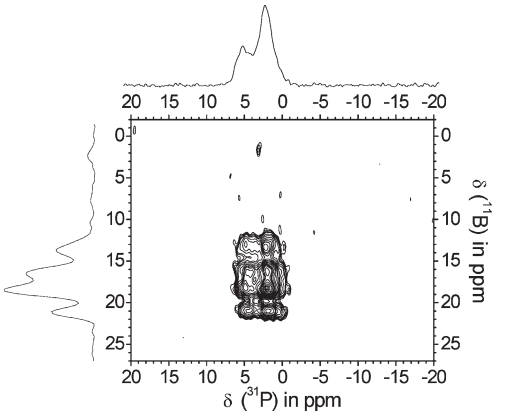

Figure 3. 2D ^{11}B−^{31}P HETCOR spectrum shown as a contour plot (center) with F2 sum projection (^{31}P dimension) on top and ^{11}B F1 sum projection on the left. Note the two phosphate signals at 2.3 ppm and 5 ppm and that no narrow HAp line appears at 2.3 ppm.

BCaP resonance is cross-polarized from the borate units, once more supporting the assumption that borate units are not contained in the crystalline HAp part. A more precise discussion is given further below (section 3.3) concerning the suggested interface between HAp and BCaP.

Figure 3 shows a ^{11}B- ^{31}P- HETCOR NMR experiment using CP. The F1 and F2 sum projections are shown on the left and on top. This shape of the 2D correlation spectrum leads to the conclusion that the various BO_3^{3-} units are randomly distributed in the phosphate network of BCaP. There is no preferential ordering to specific PO_4^{3-} sites.

The estimation of the chemical composition of the BCaP phase is a central goal of this section. A first step has been made above by estimating the relative phosphate content in the crystalline HAp. As the entire borate is in BCaP the last problem concerns the structural assignment and quantification of the ^{1}H resonances, particularly of the new −0.6 ppm signal (Figures 1 and 5). To solve this problem, 2D ^{1}H- ^{31}P HETCOR spectra were acquired for various mixing times ranging from 500 μs to 8 ms (Figure 4).

These 2D correlation spectra are dominated by the strong HAp peak at 0 ppm/2.3 ppm (in the following always: ^{1}H shift/^{31}P shift) that shows the spatial proximity of the OH^- protons to the PO_4^{3-} groups in the HAp

(22) Massiot, D.; Fayon, F.; Capron, M.; King, I.; Le Calve, S.; Alonso, B.; Durand, J. O.; Bujoli, B.; Gan, Z. H.; Hoatson, G. *Magn. Reson. Chem.* **2002**, *40*, 70.

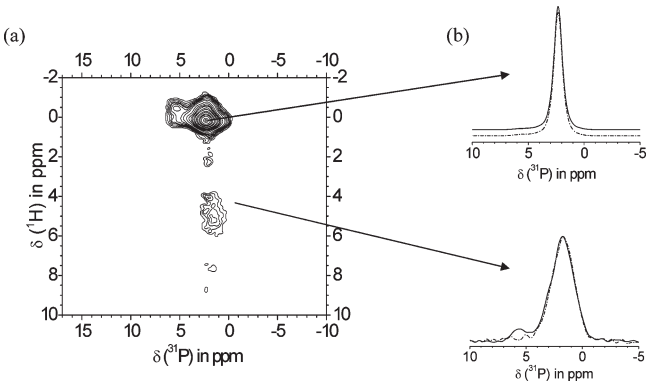

Figure 4. (a) 2D $^{1}H-^{31}P$ HETCOR spectrum with a CP contact time of 2 ms. Three correlation peaks are observed: the intense peak at 0 ppm/2.3 ppm (^{1}H vs ^{31}P shift) for crystalline HAp, a new −0.6 ppm/5.5 ppm peak (Ca−OH-type protons in BCaP), and the weak 5 ppm/1.8 ppm and 7.5 ppm/1.8 ppm correlation peaks which belong to the BCaP phase. (b) Partial F2 sum projections (normalized) across the indicated peaks (dashed lines: 2 ms, solid lines: 8 ms CP time).

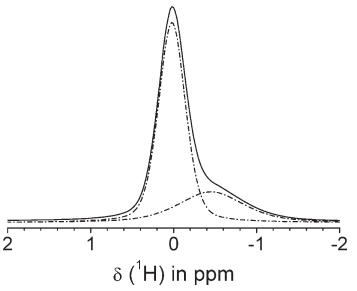

Figure 5. Line shape fit of ^{1}H MAS NMR spectrum using two lines for HAp (0 ppm) and the Ca−OH resonance of BCaP at −0.6 ppm. The intensity ratio is 72%/28%.

structure. There is another weak correlation peak at −0.6 ppm/5.5 ppm. Ca−OH type protons (cf. section 3.1) are close to phosphate units having a chemical shift of 5.5 ppm. It readily means that these protons must be in the BCaP phase and that they do not belong to the HAp structure. Furthermore, weak correlation peaks exist at 5 ppm/1.8 ppm and 7.5 ppm/1.8 ppm which are assigned to water molecules (5 ppm) and some hydrogen phosphate groups (7.5 ppm) in close spatial proximity to disordered phosphate units in BCaP (broad ^{31}P peak at 1.8 ppm). The most important result is that the BCaP phase contains Ca−OH type protons (−0.6 ppm line, Figures 1 and 5). Their relative concentration can be obtained from a fit of the line profile as shown in Figure 5. Accordingly, the BCaP structure contains about 28% of such protons compared to the stoichiometric HAp.

The chemical composition of BCaP can now be estimated using the following results/approximations:

(a) 30% of the phosphate is in HAp
(b) all borate units are located in BCaP
(c) the OH^- ratio between HAp and BCaP is 72/28
(d) small concentrations of BO_2^- and HPO_4^{2-} units and water molecules are neglected

First, the phosphate content of the crystalline HAp is subtracted from the recalculated sample composition according to the ICP data, which yields the relative BO_3^{3-} and PO_4^{3-} numbers for BCaP. The OH^- number is obtained by taking the 72%/28% ratio for HAp/BCaP as determined from the ^{1}H MAS NMR spectrum. Finally, the Ca^{2+} concentration of BCaP is calculated to ensure electric neutrality of the composition. The results are listed in Table 1, and the procedure was repeated for the 25% and 35% phosphate contents of HAp to get an error estimation for the suggested composition.

Table 1. Estimation of the BCaP Composition[a]

relative P amount of HAp ($Ca_{10}(PO_4)_6(OH)_2$)	estimated composition of BCaP
30% HAp	**$Ca_{10.26}(PO_4)_6(BO_3)_{0.72}(OH)_{0.36}$**
35% HAp	$Ca_{10.40}(PO_4)_6(BO_3)_{0.78}(OH)_{0.46}$
25% HAp	$Ca_{10.16}(PO_4)_6(BO_3)_{0.67}(OH)_{0.28}$

[a] For details see text. The compositions are calculated for a fixed number of PO_4^{3-} units (here: six) to make them comparable to the HAp stoichiometry. Bold numbers: most likely composition due to NMR line shape analysis.

3.3. Support for a "Core-Shell" Model of the Borate Containing Samples by Evidence for an Interface Layer between HAp and BCaP. It was shown in the previous sections that the sample contains crystalline HAp (verification by XRD and NMR) and a disordered borate containing BCaP phase (only by NMR). Two possibilities can be considered: either separate HAp and BCaP particles are formed simultaneously by the synthesis or both phases compose one and the same crystal. To distinguish between these two scenarios specific NMR experiments have been run. The first one ($^{11}B-^{31}P$ edited $^{31}P\{^{1}H\}$ REDOR) hints on a thin disordered HAp layer in/at the BCaP phase, whereas the second one ($^{1}H\{^{11}B\}$ TRAPDOR NMR) shows that the borate units of the BCaP phase are in spatial proximity to the crystalline HAp. Both results together can be taken as strong arguments for the suggested thin interface layer and, thus, support the "core-shell" model.

i. Thin Disordered HAp Layer around the BCaP Phase. This experiment ($^{11}B-^{31}P$ edited $^{31}P\{^{1}H\}$ REDOR) consists of two parts and pursues the following idea. The ^{31}P MAS BCaP line shape is excited by cross-polarization from the borate units ($^{11}B-^{31}P$ CP). Afterward, a $^{31}P-\{^{1}H\}$ REDOR part follows that probes the spatial proximity of protons exclusively to the phosphate groups of the BCaP structure. Figure 6a shows the rotor-synchronized ^{31}P echo line shapes of BCaP (solid and dashed lines for refocusing ^{1}H 180° pulses off and on, respectively) together with the REDOR difference spectrum (dash-dotted line) for a short dephasing time of 0.48 ms. The normalized REDOR intensity differences (amplitudes taken only) are plotted in Figure 6b where the filled triangles and circles show the REDOR effect for the 2.3 ppm and 5 ppm peaks separately. For comparison reasons $^{1}H\{^{31}P\}$ REDOR data for crystalline HAp are shown as well (solid squares).

The HAp REDOR intensities increase much quicker than those of the BCaP lines at 5 ppm and 2.3 ppm. It also looks at a first glance as if the $^{31}P-^{1}H$ heteronuclear dipole coupling for the 5 ppm line is smaller than that of the broad 2.3 ppm BCaP resonance because the

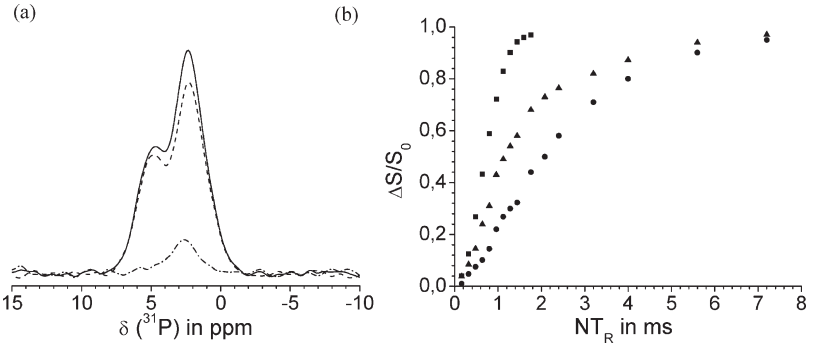

Figure 6. ^{11}B−^{31}P edited ^{31}P{^{1}H} REDOR: (a) ^{31}P echo spectra for ^{1}H 180° pulses switched off (solid line) and switched on (dashed line) and difference spectrum (dash-dotted line) for a dephasing time of 0.48 ms; (b) normalized REDOR difference intensities of the ^{11}B−^{31}P CP edited 2.3 ppm (triangles) and 5 ppm (circles) lines of the BCaP phase. Experimental data (squares) for crystalline HAp are plotted for comparison. For details see text.

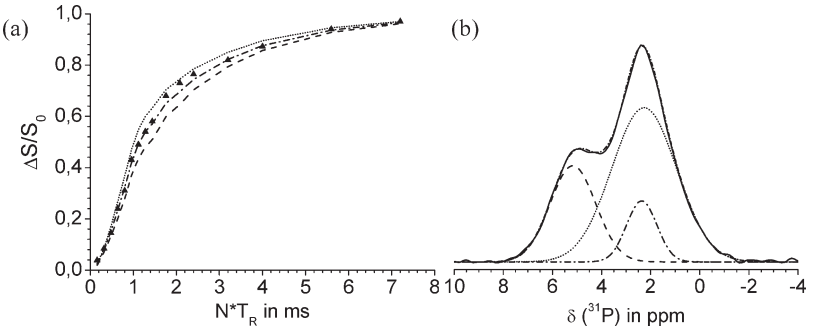

Figure 7. (a) Approximation of the REDOR curve of the ^{11}B−^{31}P CP edited broad ^{31}P resonance at 2.3 ppm as being composed of REDOR components of a "HAp-like" part and of the BCaP (5 ppm line was taken). Best approximation (dash-dot) is obtained for 14% ("HAp-like") and 86% (5 ppm BCaP data), respectively. The other approximations show the combination 10%/90% (dashed) and 20%/80% (dotted) which are clearly worse. (b) Fit of ^{11}B−^{31}P CP spectrum with the two broad ^{31}P BCaP peaks and the narrower ^{31}P line at 2.3 ppm for the "HAp-like" structural motif.

corresponding REDOR curve lies between the HAp and 5 ppm BCaP data. However, a closer inspection of the experimental REDOR spectra leads to a different interpretation:

(i) For short dephasing times (up to about 0.48 ms) a narrow REDOR difference spectrum is found in the 2.3 ppm region as shown in Figure 6a, and this ^{31}P{^{1}H} REDOR difference spectrum is distinctly narrower than the 2.3 ppm ^{31}P BCaP peak!

(ii) This remarkable line shape difference between the REDOR difference spectrum and the ^{31}P echo line shape vanishes, though, for REDOR dephasing times longer than about 1 ms. Now, the ^{31}P BCaP line shapes of the two REDOR measurements with the ^{1}H 180° pulses off and on have the same shape!

(iii) These findings apply only for the 2.3 ppm ^{31}P BCaP resonance, not for the 5 ppm line.

These facts (narrow line around 2.3 ppm found for the short REDOR time of about 0.48 ms, but it vanishes after 1 ms) can be explained using the ^{31}P{^{1}H} REDOR data of a HAp reference sample (Figure 6b). The HAp REDOR curve shows that any HAp signal with the dephasing ^{1}H 180° pulses switched on will vanish for times longer than 1 ms. For shorter times, the corresponding signal is found. This is the explanation for the change in the REDOR difference line shapes for this sample. In other words, it is suggested that the ^{31}P{^{1}H} REDOR behavior of the total 2.3 ppm BCaP line can be considered as a superposition of a "HAp-like" term (determines the short time behavior) and the "typical" BCaP behavior that is found in the 5 ppm REDOR data. This assumption leads to very good approximation of the 2.3 ppm REDOR data (Figure 7a). The best agreement is obtained taking 14% for the quick "HAp-like" component and 86% of the BCaP data of the 5 ppm line.

The precise phosphate ratio for these components can be obtained by line shape procedure as shown in Figure 7b. This fit shows the two broad ^{31}P BCaP peaks and the narrower ^{31}P line at 2.3 ppm. The latter has only about 11% of the total BCaP phosphate content. Furthermore, the line width of this narrow 2.3 ppm line is about a factor of 2 broader compared with the HAp line shape obtained in this sample using the ^{1}H−^{31}P CP as shown in Figure 8. In conclusion, the ^{31}P line shape of BCaP contains, to a minor part of about 11%, phosphate units that have a similar REDOR behavior like HAp. It is suggested that a "HAp-like" part is present in the BCaP phase, and it is considered to be disordered because of the line width compared to the crystalline HAp phase. It is likely that it forms an interface.

ii. BCaP Borate Units Are in Spatial Proximity to the Crystalline HAp Phase. The proposal of such an interface needs further support. ^{1}H{^{11}B} TRAPDOR measurements have been carried out to test spatial proximities of different types of protons (OH^-, H_2O) to the borate units. The experimental data are plotted in Figure 9. The

echo detected ^{1}H spectrum (single rotor period prior to the 180° ^{1}H echo pulse) is shown by the solid line. The dashed and dashed-dotted lines represent the TRAPDOR difference signals for two different times, 2.56 and 5.76 ms, respectively. Their line shapes are compared normalized in Figure 9b for the 0 ppm region. The interesting result is that these TRAPDOR difference lines consist of two components. The −0.6 ppm $^{1}H\{^{11}B\}$ TRAPDOR signal is expected because it is caused by Ca−OH type protons in the borate containing BCaP part (cf. section 3.1 and 3.2). This signal is most prominent in the TRAPDOR experiment with the short time. But the other 0 ppm signal does not makes sense at first glance because it seems to be the OH^{-} resonance of HAp that is not part of the BCaP phase as shown earlier. If so, no TRAPDOR effect can be expected. However, this 0 ppm TRAPDOR signal does have a larger line width compared with the strong HAp signal (solid line) as seen in Figure 9b. Furthermore, the intensity of the 0 ppm TRAPDOR signal increases for longer TRAPDOR times and, simultaneously, its line width decreases slightly. And its line width is always larger than the HAp line.

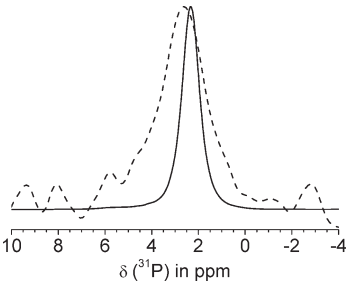

Figure 8. ^{31}P line shape comparison for the crystalline HAp phase in this sample ($^{1}H-^{31}P$ CPMAS spectrum, solid line) and $^{11}B-^{31}P$ edited $^{31}P-\{^{1}H\}$ REDOR difference spectrum (dashed line) for a dephasing time of 0.48 ms.

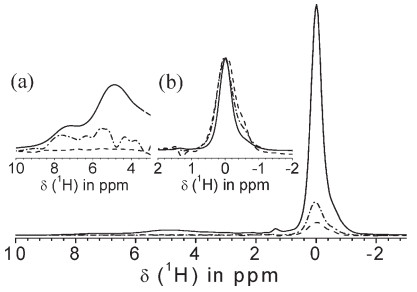

Figure 9. $^{1}H\{^{11}B\}$TRAPDOR NMR: Bottom: ^{1}H MAS NMR spectrum (solid line) in comparison $^{1}H\{^{11}B\}$TRAPDOR difference spectra for a dephasing time of 2.76 ms (dashed line) and 5.76 ms (dashed-dotted line). Inset (b): normalized spectra in the 0 ppm region. Inset (a): ^{1}H MAS NMR line in comparison with eight times magnified TRAPDOR difference lines. TRAPDOR effects are only visible for this magnification suggesting either larger distances between the water molecules and borate units or increased mobility.

The remarkable result is taken as another hint on a "HAp-like" interface layer between BCaP and crystalline HAp. It may readily explain why these few HAp type interface protons "see" the borate units in the BCaP phase. Also, the TRAPDOR line at 0 ppm is about 1.5 times broader than the ^{1}H line of the crystalline HAp suggesting a "disordered" HAp type interface. This interpretation supports the REDOR data explained earlier. And finally, the longer the TRAPDOR time is, the more ordered the ^{1}H TRAPDOR signal at 0 ppm appears hinting on a quite thin interface layer toward the crystalline HAp.

It was found that about 11% of the BCaP phosphate content must be attributed to a disordered "HAp-like" interface layer. As BCaP and interface together contain about 70% of the entire phosphate it can be estimated that the interface itself contains approximately 8% of the phosphate leaving 62% for the BCaP.

4. Conclusions

These NMR investigations gave clear evidence that this borate substituted calcium phosphate sample consists of crystalline HAp and a disordered BCaP phase. The chemical composition of the latter could be estimated from the quantified NMR spectra. It has further been shown that various results of NMR measurements hint on the presence of an interface layer between HAp and BCaP. This means that the borate containing calcium phosphate particles contain both phases, and one can exclude that separate HAp and BCaP particles have been synthesized. In this context we refer to previously published results of the structure of HAp[13] where it was

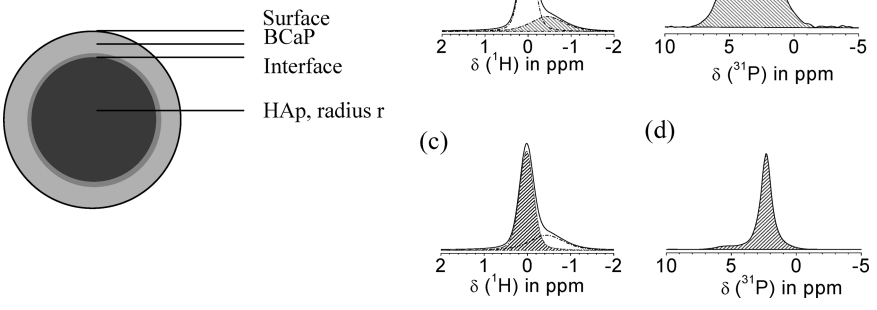

Figure 10. Sketch of the borate containing calcium phosphate particles having a crystalline core of stoichiometric HAp covered by a surface layer of BCaP with about 49% thickness of the core radius *r* and a thin HAp type interface layer (8% of the core radius). Typical ^{1}H and ^{31}P NMR spectra of the core (c, d) and the surface region (a, b) are shown hatched, respectively.

shown that even in nanocrystalline HAp only part of the phosphate forms stoichiometric HAp. There, a model was proposed that HAp forms the core of the particles and that this crystalline HAp core is covered by a thin and disordered surface layer with a different chemical composition, thus explaining the well-known Ca^{2+} deficiency; meanwhile it was confirmed by other groups.[14]

The suggestion here is that the disordered BCaP phase covers the crystalline HAp phase as core of the particles and not vice versa. The quantitative result given in section 3 can be summarized as follows:

(i) ca. 30% phosphate is in HAp core
(ii) ca. 8% phosphate is in interface, distorted HAp
(iii) ca. 62% phosphate in BCaP, surface layer

These numbers can be used for an estimation of the relative thicknesses for simple particle geometries. Taking, for example, a sphere and assuming further that the densities of HAp and BCaP are similar, the relative phosphate ratio for the two phases can be used to estimate the radii for the core (HAp), the interface layer, and the shell thickness (BCaP). Given the radius for the HAp core is r (with 30% of the entire phosphate), then the interface layer thickness amounts to about 8% of the HAp core radius r. HAp and interface layer together contain 38% of the phosphate. The outer BCaP layer thickness is then 49% of the core radius r. To give an example, if the HAp core radius is, say, 100 nm, the interface thickness is about 8 nm, whereas the surface BCaP layer is about 49 nm thick. Figure 10 summarizes these results and shows the typical NMR signals for the HAp core and the BCaP surface layer, taken from specific NMR experiments.

It is clear that the knowledge about the structure of (disordered) surfaces plays a key role for the understanding of properties like potential bioactivity and biodegradability of such materials. This piece of information is essential for the assessment and new design of bone substitutes or scaffolds for bone regeneration. Especially, the surface chemistry of biomaterials is important for regulating the adsorption of proteins and cell adhesion. We finally mention that the proposed structural model of this borate containing calcium phosphate prepared by a high-temperature solid state reaction can explain preliminary dissolution rate data of biodegradation investigations measured by the change for the Ca^{2+} concentration as function of time in acetic acid and sodium acetate buffer solution (pH = 5.5, model of osteoclastic resorption according to ref 23). Further work is in progress.

Acknowledgment. This work has been supported by the Deutsche Forschungsgemeinschaft DFG under the JSPS-DFG scheme (Grant Ja 552/25-1) and by a Grant-in-Aid for Scientific Research from the Japan Society for the Promotion of Science under the JSPS-DFG scheme.

Supporting Information Available: ICP-data, information about specific surface area, FT-IR spectrum, and XRD analysis of the boron containing calcium orthophosphate sample (PDF). This material is available free of charge via the Internet at http://pubs.acs.org.

(23) Ito, A.; Senda, K.; Sogo, Y.; Oyane, A.; Yamazaki, A.; LeGeros, R. Z. *Biomed. Mater.* **2006**, *1*, 134.